Rev. Adv. Mater. Sci. 39 (2014) 84-91

CRACK GENERATION INITIATED BY NANOSCALE IDEAL SHEAR IN CRYSTALLINE, NANOCRYSTALLINE AND METAL-CERAMIC NANOCOMPOSITE SOLIDS

I.A. Ovid'ko[1,2] and A.G. Sheinerman[1,2]

[1]St. Petersburg State Polytechnical University, St. Petersburg 195251, Russia
[2]Department of Mathematics and Mechanics, St. Petersburg State University, St. Petersburg 198504, Russia

Received: October 03, 2014

Abstract. A new special mechanism of crack generation in single-phase crystalline, nanocrystalline and metal-ceramic nanocomposite solids deformed at ultrahigh stresses is suggested and theoretically examined. Crack generation is preceded by homogeneous formation of a nanoscale configuration of three non-crystallographic partials whose Burgers vector magnitudes continuously grow during the formation process at high shear stresses. Then a crack is generated at the dislocation with the largest Burgers vector magnitude. It is shown that cracks can be effectively generated by this mechanism in Ni (nickel), 3C-SiC (the cubic phase of silicon carbide) and metal-ceramic nanocomposites deformed at ultrahigh stresses.

1. INTRODUCTION

Nanocrystalline materials show unique mechanical characteristics (superior strength, etc.) that represent the subject of intensive research efforts; see, e.g., reviews [1–14]. The unique characteristics are associated with non-conventional plastic flow mechanisms operating in nanomaterials; see, e.g., reviews [1–14] and research papers [15–20]. In particular, the action of standard dislocation sources (like Frank-Read ones) is suppressed by nanoscale and grain boundary (GB) effects in nanomaterials, and GBs serve as obstacles for lattice dislocation slip. In this situation, quasistatic plastic deformation of nanomaterials is hampered and occurs at stresses highly exceeding those causing plastic deformation of their coarse-grained counterparts (e.g., [1–14]). Very high stresses often initiate fast generation and growth of cracks in nanomaterials which thereby tend to show the brittle fracture behavior. The discussed behavioral features of nanomaterials at a quasistatic mechanical load are, in part, similar to those of conventional crystalline (coarse-grained polycrystalline and single crystalline) solids deformed at high-strain-rate and indenter load regimes. Shock wave deformation of crystalline solids commonly occurs at extra high stresses, involves non-standard mechanisms for lattice dislocation nucleation and plastic flow, and often initiates brittle cracks [21]. In particular, following Meyers [21], the action of ultrahigh shear stresses near the shock wave front is capable of causing homogeneous *local* nucleation of lattice dislocations. In the two-dimensional model picture of this process, two lattice dislocations of opposite Burgers vectors nucleate at one point and slip over short distances in opposite directions [21] (Figs. 1a-1d). Dislocations nucleating in the homogeneous way are viewed to crucially contribute to plastic flow near the shock wave front [21].

Corresponding author: I.A. Ovidko, e-mail: ovidko@nano.ipme.ru

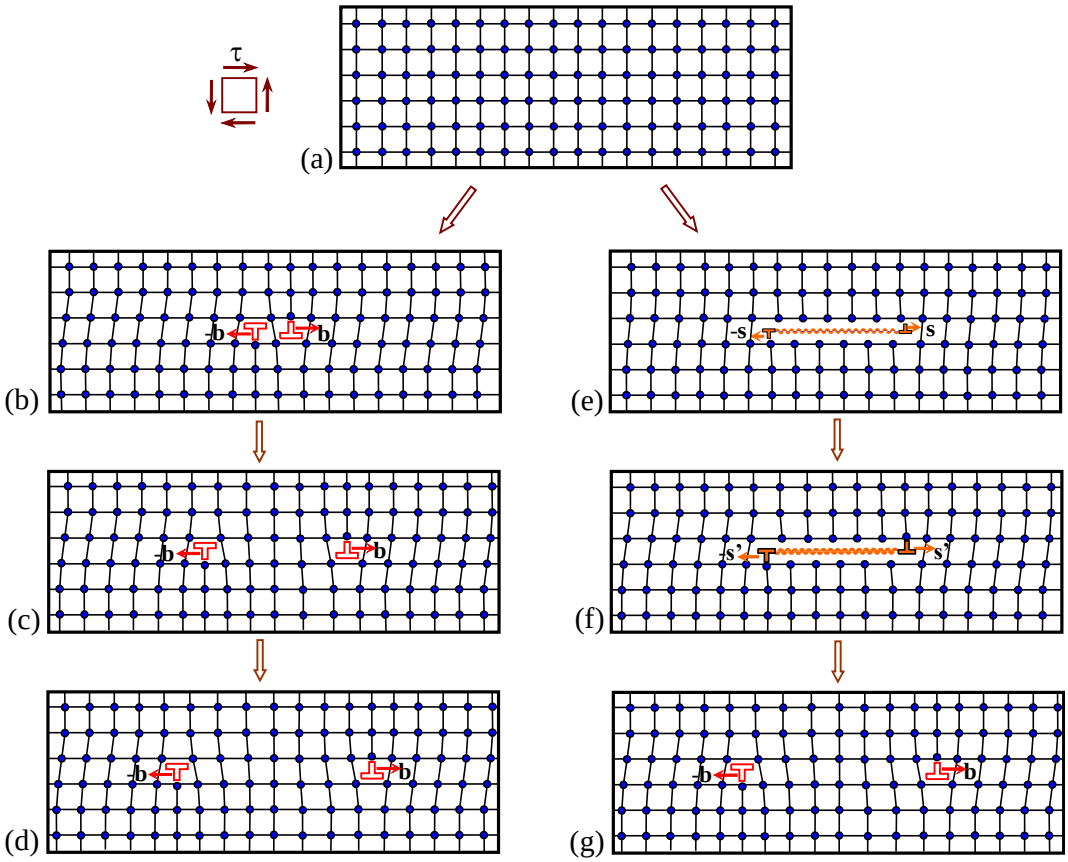

Fig. 1. Local (a-d) and non-local (a, e-g) generation of a dislocation dipole under the action of an ultrahigh stress. Local generation of a dislocation dipole implies generation of a dipole of lattice dislocations at close proximity to each other followed by an increase of the distance between the dislocations. Non-local generation of a dislocation dipole involves the generation of a dipole of non-crystallographic dislocations with small Burgers vector magnitudes (joined by a generalized stacking fault). In this process, the magnitude of the dislocation Burgers vectors increase and eventually reaches that of lattice dislocation Burgers vectors. The wavy line represents the generalized stacking fault between dislocations with non-crystallographic Burgers vectors.

Recently, it has been suggested that homogeneous *non-local* nucleation of lattice dislocations occurs in nanocrystalline materials [22], nanocomposites [23], nanoscale films [24,25], nanowires [26,27], and Gum Metals [28]. (In doing so, in the two-dimensional case, two non-crystallographic partial dislocations nucleate by a nanoscale ideal shear at two points joined by a generalized stacking fault, while their Burgers vector magnitude continuously grows (from 0) during the nucleation process [22–28] (Figs. 1a, 1e-1g). Recently, this process in titanium alloys has been experimentally documented in “in situ” observations by high-resolution electron microscopy [29]. In these materials, the homogeneous *non-local* nucleation in nanomaterials occurs at a stress level lower than that causing the homogeneous *local* nucleation of dislocations. In the context discussed, one expects that homogeneous *non-local* nucleation of lattice dislocations can occur near the shock wave front in crystalline, nanocrystalline and nanocomposite solids. With the dominant role of dislocations generated in the (*local* and/or *non-local*) homogeneous way in high-strain-rate deformation, these dislocations are expected to cause strong effects on fracture of crystalline, nanocrystalline and nanocomposite solids deformed at high stresses. Similar processes and effects can occur at high stresses generated in solids under indenter loading. The main aim of this paper is to suggest and theoretically describe a new mechanism for crack nucleation involving *non-local* homogeneous processes of dislocation nucleation in GBs, interphase boundaries and grain interiors of crystalline, nanocrystalline and metal-ceramic nanocomposite solids deformed at ultrahigh stresses.

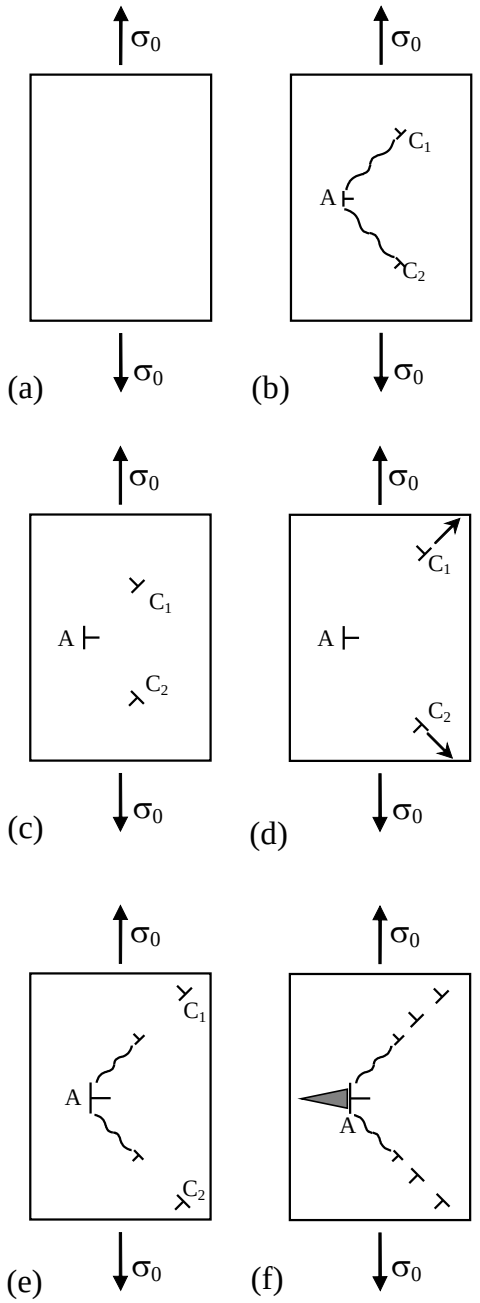

Fig. 2. Formation of a dislocation with a large Burgers vector and crack in a deformed solid as a result of ideal local shears. (a) Initial dislocation-free state. (b) Dislocation A, B and C with growing Burgers vectors are formed in the deformed solid. Dislocations B and C are joined with dislocation A by stacking faults. (c) The Burgers vectors magnitudes of dislocations A, B and C reach those of lattice dislocations. As a result, stacking faults disappear. (d) Under the action of the applied stress, dislocations B and C move away from dislocation A. (e) New dislocations with growing Burgers vectors nucleate by local shears. The Burgers vector magnitude of dislocation A increases. (f) A crack nucleates at dislocation A.

2. GEOMETRY OF CRACK GENERATION INITIATED BY NANOSCALE IDEAL SHEAR IN SOLIDS

Let us consider the geometric aspects of the special mechanism for crack generation involving *non-local* homogeneous processes of dislocation nucleation in crystalline (single crystalline and coarse-grained polycrystalline) solids deformed at ultrahigh stresses. For simplicity, we consider here the model case where the specimen is under a uniaxial tensile load σ_0, although our analysis can be extended to more typical situations of uniaxial compression or more complicated stress states typical of shock loading. The only requirement in all the cases is the action of high shear stresses at different dislocation slip planes during mechanical loading. Within our model, the mechanism for crack generation is realized as a two-stage process (Fig. 2) in a region where high shear stresses operate. In its initial state, the region is free from any defects (Fig. 2a). The first stage of the mechanism represents the *non-local* homogeneous nucleation of a nanoscale configuration of three non-crystallographic partials whose Burgers vector magnitudes continuously grow during the nucleation process at ultrahigh shear stresses near the shock wave front (Figs. 2b–2d). Then a crack is generated at the dislocation with the largest Burgers vector magnitude (Fig. 2e).

As to more details, at the first stage, the shear stress τ induces the homogeneous generation of three edge dislocations, A, C_1, and C_2, through ideal nanoscale shears (Fig. 2b). This mechanism has been considered in detail in Refs. [22–28]. In spirit of the approach [22–28], the dislocations A, C_1, and C_2 are characterized by Burgers vector magnitudes B, s_1, and s_2, respectively, that gradually increase (from 0) during their formation process (Fig. 2b). The dislocations C_1 and C_2 are connected with dislocation A by two planar defects called generalized stacking faults. According to the dislocation charge conservation law, the total Burgers vector of the three dislocations is equal to zero. Let the dislocations form in two planes symmetric about the plane normal to the tension direction. We assume that under the action of a very high shear stress the Burgers vectors of the dislocations increase until their magnitudes become equal to the magnitudes of the Burgers vectors of a lattice dislocation, and the stacking faults that join dislocations C_1 and C_2 with dislocation A disappear (Fig. 2c). After that, dislocations C_1 and C_2 move away from dislocation A

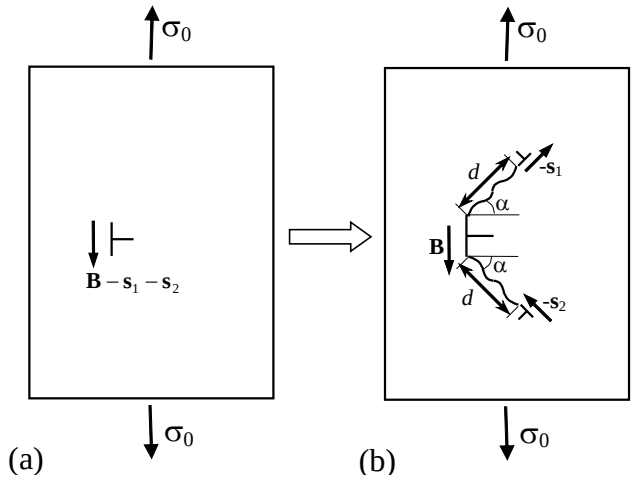

Fig. 3. Geometry of the dislocation reaction in a deformed crystalline solid. A dislocation with the Burgers vector **B**-$\mathbf{s}_1$-$\mathbf{s}_2$ (a) transforms into the dislocation with the Burgers vector **B** joined by generalized stacking faults with the dislocations with the Burgers vector -$\mathbf{s}_1$ and -$\mathbf{s}_2$ (b).

(Fig. 2d). The above process sequentially repeats (Fig. 2e) and eventually results in the formation of a dislocation A with a large Burgers vector. When the Burgers vector magnitude of dislocation A becomes large enough, a crack nucleates at this dislocation (Fig. 2f). Thus, sequential formation of dislocations with increasing Burgers vectors under an ultrahigh shear stress can lead to the generation and subsequent growth of a crack.

In order to calculate the conditions for crack generation, we consider a mechanically loaded solid containing a dislocation with the Burgers vector **B**-$\mathbf{s}_1$-$\mathbf{s}_2$ directed as shown in Fig. 3a. We suppose that the shear stress forces this dislocation to 'emit' two non-crystallographic dislocations with the Burgers vectors -$\mathbf{s}_1$ and -$\mathbf{s}_2$, connected by stacking faults with the pre-existent dislocation. As a result, the dislocation with the Burgers vector **B**-$\mathbf{s}_1$-$\mathbf{s}_2$ transforms into the dislocation with the Burgers vector **B**, connected by stacking faults with the dislocations having the Burgers vectors -$\mathbf{s}_1$ and -$\mathbf{s}_2$ (Fig. 3b). The magnitudes of the Burgers vectors -$\mathbf{s}_1$ and -$\mathbf{s}_2$ are assumed to be identical, they are designated by s, the length of stacking faults is specified by d, and the angle between the Burgers vectors -$\mathbf{s}_1$ and -$\mathbf{s}_2$ and the plane normal to the load direction is denoted as α. Then the magnitude of the Burgers vector **B**-$\mathbf{s}_1$-$\mathbf{s}_2$ equals to B-2s sinα.

3. ENERGY AND STRESS CHARACTERISTICS OF CRACK GENERATION THROUGH NANOSCALE IDEAL SHEAR IN CRYSTALLINE AND NANOCRYSTALLINE METALS AND CERAMICS

In our analysis of the dislocation reaction illustrated in Fig. 3, we assume that this reaction can occur if it is energetically beneficial and calculate the energy variation ΔW associated with the dislocation reaction. The energy variation ΔW is defined as the difference of the system energies after the dislocation reaction (see Fig. 3b) and prior to it (Fig. 3a). In the elastically isotropic case, the energy ΔW (per unit length of dislocations) is calculated as

$$\Delta W = \frac{D}{2}\left\{\left(B-2\sin\alpha\right)^2 \ln\frac{B-2s\sin\alpha}{B} + 4s\left(B-2s\sin\alpha\right)\sin\alpha\left(\ln\frac{d}{B}+1\right)+ \right.$$
$$\left. 2s^2\left[1+\cos 2\alpha \ln\frac{2d\sin\alpha}{s} + 2\sin^2\alpha\left(1+2\ln\frac{d}{s}-\ln\frac{B}{s}\right)\right]\right\} - \sigma_0 sd\sin 2\alpha + 2\gamma_{sf}(p)d, \quad (1)$$

where $D = G/[2\pi(1-\nu)]$, G is the shear modulus, ν is Poisson's ratio, $p = s/b$, b is the magnitude of the elementary Burgers vector of a lattice dislocation in a non-stressed lattice, and $\gamma_{sf}(p)$ is the energy of the generalized stacking fault per its unit area. The energy change associated with the first dislocation reaction (characterized by the formation of dislocations -$\mathbf{s}_1$ and -$\mathbf{s}_2$ joined by stacking faults with the dislocation $\mathbf{s}_1$+$\mathbf{s}_2$) is equal to $\Delta W(B = 2s\sin\alpha)$.

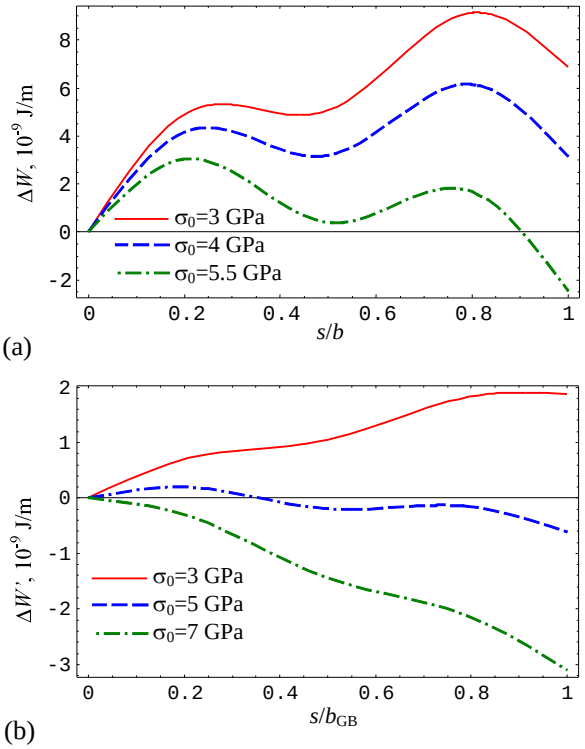

Fig. 4. The energy variations ΔW (a) and $\Delta W'$ (b) associated with the emission of lattice (a) and grain boundary (b) dislocations by ideal local shears vs. the normalized magnitudes s/b (a) and s/b_{GB} (b) of the dislocation Burgers vectors.

Let us plot the dependences $\Delta W(s/b)$ for the exemplary case of Ni characterized by the following values of parameters: G = 73 GPa, ν = 0.34, and b = 0.25 nm. For Ni, the dependence $\gamma_{sf}(p)$ has been found to be as follows [30]:

$$\gamma_{sf}(p)=\begin{cases}\gamma_m \sin 2\pi p, & p<\dfrac{1}{4},\\ \dfrac{\gamma_m+\gamma_0}{2}-\dfrac{\gamma_m-\gamma_0}{2}\cos 4\pi p, & \dfrac{1}{4}\le p<\dfrac{3}{4},\\ -\gamma_m \sin 2\pi p, & \dfrac{3}{4}\le p\le 1.\end{cases} \quad (2)$$

For definiteness, we put $\alpha = \pi/4$, and d = 15 nm. The dependences $\Delta W(s/b)$ for different values of σ_0 are shown in Fig. 4a. As it follows from Fig. 4a, the dependences $\Delta W(s/b)$ have complicated characters. It is seen that the dislocation reaction requires overcoming an energetic barrier. This energetic barrier is absent in the case of a very high stress σ_0 (11.5 GPa or more). However, this stress exceeds the theoretical fracture stress for Ni and, therefore, this case is not shown in Fig. 4a. To estimate the critical stress for the formation of lattice dislocations by local shears, we assume that this process is possible if $\Delta W(p = 1) \le 0$ and $(\partial \Delta W/\partial p)|_{p=1} \le 0$. In this case, the dislocation reaction requires overcoming an energetic barrier. We assume that this energetic barrier can be surmounted through thermal fluctuations during mechanical loading. Then for the case $\alpha = \pi/4$ and d = 15 nm, these conditions are satisfied if $\sigma_0 > 4.9$ GPa and $\sigma_0 > 7.9$ GPa, at B = 0.7 nm and B = 1.5 nm, respectively.

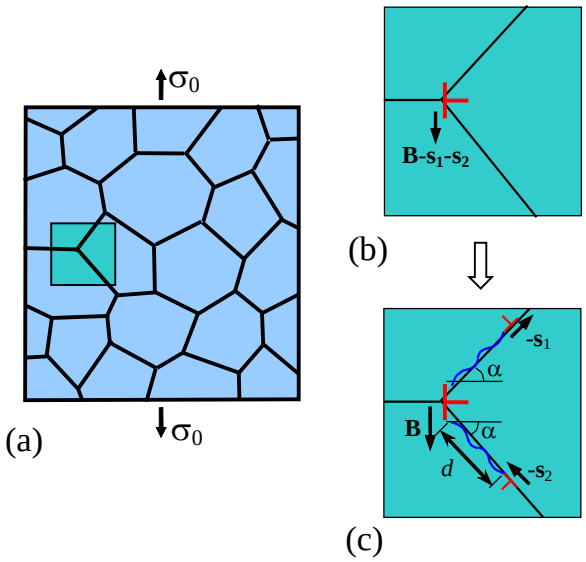

Fig. 5. Geometry of the dislocation reaction in a deformed nanocrystalline solid. (a) Nanocrystalline solid under a tensile load (general two-dimensional view). (b,c) A dislocation with the Burgers vector **B**-**s**$_1$-**s**$_2$ (b) transforms into the dislocation with the Burgers vector **B** joined by grain boundary generalized stacking faults with the dislocations with the Burgers vector -**s**$_1$ and -**s**$_2$ (c).

We now consider nanocrystallne materials containing large amounts of grain boundaries (GBs) and their triple junctions. In nanocrystalline materials, there is a typical situation where dislocations with the Burgers vectors -**s**$_1$ and -**s**$_2$ are generated at GBs (Fig. 5). In doing so, the Burgers vectors of the dislocations formed due to ideal nanoscale shears increase until their magnitudes reach the magnitude b_{GB} of the Burgers vector of GB dislocations ($b_{GB} \approx b/3$). In order to calculate in a first approximation the energy $\Delta W'(s/b_{GB})$ characterizing the formation of a dipole of non-crystallographic GB dislocations, we use the expression for $\Delta W'(s/b)$, where we replace b by b_{GB} and multiply the specific energy $\gamma_{sf}(s/b_{GB})$ of the stacking fault by a factor of 0.1. The introduction of the latter factor accounts for the fact that the energy of a stacking fault in a GB is much smaller than in a grain interior.

The dependences $\Delta W'(s/b_{GB})$ for Ni with $\alpha = \pi/4$, B = 0.7 nm, d = 15 nm and different values of σ_0

are shown in Fig. 4b. As is seen in Fig. 4b, if the stress σ_0 is not too high, the dislocation reaction requires surmounting an energetic barrier (see the two upper curves in Fig. 4b). However, for high enough stress, this reaction can occur in a non-barrier way (see the lowest curve in Fig. 4b). For the parameter values used in Fig. 4b, the non-barrier dislocation formation by local shears is possible at σ_0>6.3 GPa. Considering the formation of GB dislocations by local shears, we assume, as previously, that this process is possible if $\Delta W'(s/b_{GB}=1) \le 0$ and $(\partial \Delta W'/\partial(s/b_{GB}))|_{s/b_{GB}=1} \le 0$. For the case Ni with $\alpha = \pi/4$ and d = 15 nm, these conditions are satisfied if $\sigma_0 > 4.2$ GPa and $\sigma_0 > 7.4$ GPa, at B = 0.7 nm and B = 1.5 nm, respectively.

The conditions for the formation of local shears have also been performed for 3C-SiC characterized by the following parameter values: G = 160 GPa, ν = 0.45, and b = 0.435 nm. Since the specific stacking fault energy for 3C-SiC is extremely low ($\gamma_0 = 10^{-4}$ J/m^2 [31]), the energy $\gamma_{sf}(p)$ of the generalized stacking fault can be neglected for this material. Then, for $\alpha = \pi/4$, $B = 2b\sqrt{2}$ = 1.23 nm, and d = 15 nm, we obtain that the formation of lattice dislocations by local shears is possible if $\sigma_0 > 28$ GPa. This stress exceeds the theoretical fracture strength for 3C-SiC, and so the formation of lattice dislocations by local shears in 3C-SiC is not likely. At the same time, the formation of GB dislocations by local shears in nanocrystalline 3C-SiC is possible if $\sigma_0 > 17$ GPa. This stress level is also extremely high but can possibly be reached in 3C-SiC in the course of shock loading.

Now let us calculate the conditions at which the generation of the crack (Fig. 1e) formed at a dislocation with a large Burgers vector **B** (formed as shown in Figs. 2 and 4) is energetically favored. We consider the situation where a high mechanical load creates a dislocation with a large magnitude of the Burgers vector, after which the load is removed. Note that very high shear stresses typically operate at deformation tests (high-strain-rate deformation, indenter load, high-pressure load in diamond anvils) related to high-stress compression that hinders crack generation. However, for a short time period immediately after the deformation test, the dislocations with large Burgers vectors are logically assumed to exist (Fig. 1d) and initiate cracks (Fig. 1e). In order to calculate the conditions at which the crack generation (Fig. 1e) is energetically favored, we use the energy criterion of crack growth [24]. Then the growth of the crack is energetically beneficial, if the crack length l is smaller than its equilibrium length l_e ($l < l_e$), where

$$l_e = \frac{GB^2}{8\pi(1-\nu)\gamma_e}. \qquad (3)$$

$\gamma_e = \gamma$ for an arbitrary crack in a ceramic and an intragrain crack (GB crack) in a metal, and $\gamma_e = \gamma - \gamma_b/2$ for a GB crack in a metal, γ is the specific surface energy, and γ_b is the GB energy per its unit area. The term $\gamma_b/2$ appears in formula (3) because GB cracks in metals are supposed to remove a fragment of GB characterized by excess specific energy γ_b. For Ni, we have: $\gamma \approx 2$ J/m^2, $\gamma_b = 0.69$ J/m^2. With these values of γ and γ_b, we obtain for the case of a GB crack that at B = 0.7 nm, l_e = 1.3 nm. In this case, the equilibrium crack length is extremely small. However, in the case B=1.5 nm, one obtains: l_e = 6 nm, so that the equilibrium crack length substantially increases. For a GB crack in 3C-SiC, at B = 1.23 nm, $\gamma \approx 2$ J/m^2 (an estimate of surface energy for 6H-SiC [33]) and $\gamma_b = 0/8$ J/m^2, we have l_e = 11 nm. This means that dislocations with large Burgers vectors formed during mechanical loading can induce the formation of nanocracks that can promote further fracture of the nanocrystalline solid.

4. ENERGY AND STRESS CHARACTERISTICS OF CRACK GENERATION THROUGH NANOSCALE IDEAL SHEAR IN METAL-CERAMIC NANOCOMPOSITES

We now consider crack generation through nanoscale ideal shear in metal-ceramic nanocomposites having two typical structures (see, e.g., [1,3,34,35]): nanocrystalline nanocomposites containing metallic and ceramic nanograins (Fig. 6), and microcrystalline-metal-matrix nanocomposites containing ceramic nanoparticles at GBs (Fig. 7). In these situations, non-crystallographic dislocations having the Burgers vectors-$\mathbf{s}_1$ and -$\mathbf{s}_2$ are generated at interphase boundaries (Figs. 6 and 7). For the estimates of the energy and stress characteristics of the crack generation through nanoscale ideal shear in metal-ceramic nanocomposites, one needs to know the energy of generalized stacking faults within interphase boundaries. In general, metal-ceramic interphase boundaries carry both dilatation and orientation mismatches between adjacent crystallites. Such boundaries possess very different structures and thereby are specified by widely varying values of the generalized stacking fault energy $\gamma_{SF\text{-}IB}$ (being highly sensitive to the interphase boundary structure). In this case, for the aims of this paper,

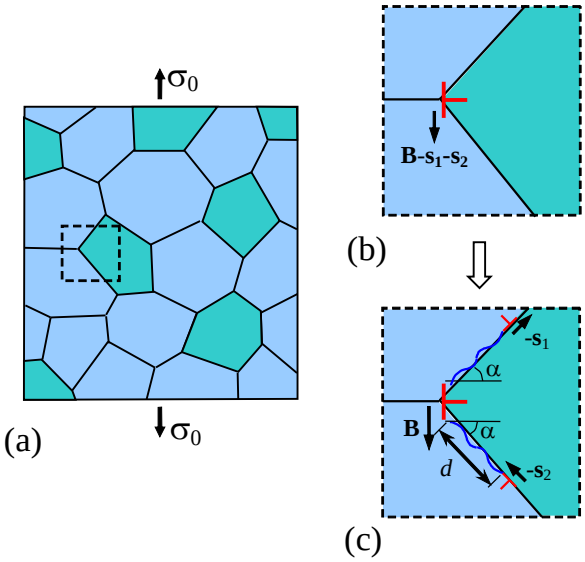

Fig. 6. Geometry of the dislocation reaction in a deformed nanocrystalline nanocomposite containing metallic and ceramic nanograins. (a) Nanocrystalline nanocomposite under a tensile load (general two-dimensional view). (b,c) A dislocation with the Burgers vector **B**-**s**$_1$-**s**$_2$ (b) transforms into the dislocations with the Burgers vectors **B**, -**s**$_1$ and -**s**$_2$ (c).

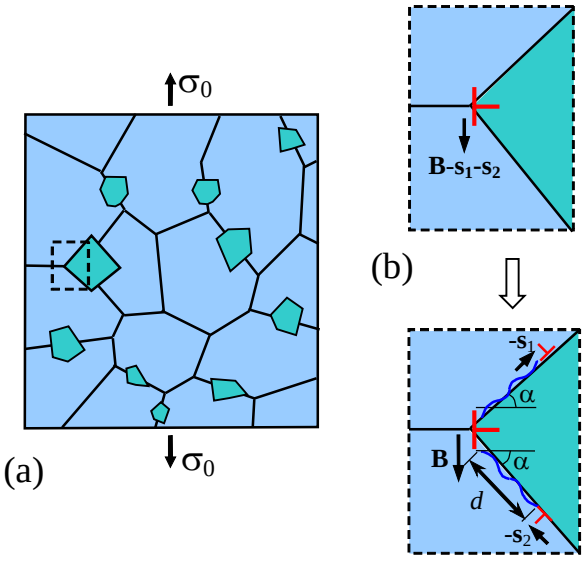

Fig. 7. Geometry of the dislocation reaction in a deformed microcrystalline-metal-matrix nanocomposite containing ceramic nanoparticles at grain boundaries. (a) Microcrystalline-metal-matrix nanocomposite under a tensile load (general two-dimensional view). (b,c) A dislocation with the Burgers vector **B**-**s**$_1$-**s**$_2$ (b) transforms into the dislocation with the Burgers vectors **B**, -**s**$_1$ and -**s**$_2$ (c).

we will use the following approximate estimates for the energy in question: $\gamma_{SF\text{-}IB} = m\gamma_{sf}$, where the factor m is in range from 0.05 to 2, and γ_{sf} is the generalized stacking fault energy in the metallic phase. For simplicity, in a first approximation, we will also characterize metal-ceramic nanocomposites as isotropic solids characterized by averaged elastic moduli. To do so, we will employ the Reuss approximation, where the effective Young moduus of a metal–ceramic nanocomposite is given as follows (e.g., [36]): $E=E_1E_2/(E_1\rho_2 + E_2\rho_1)$. Here E_1 and E_2 are the Young moduli of the metal and ceramic phase, respectively, while ρ_1 and ρ_2 are the volume fractions of the metal and ceramic phases. Similarly, we introduce the effective Poisson's ratio as $\nu = (\nu_1\rho_1E_2 + \nu_2\rho_2E_1)/(E_1\rho_2 + E_2\rho_1)$, where ν_1 and ν_2 are Poisson's ratios of the metal and ceramic phase, respectively.

We now focus on the case of Ni–3C-SiC (metal-ceramic) nanocomposites. For definiteness, we put $\rho_1 = 0.7$ and $\rho_2 = 0.3$ and $\alpha = \rho/4$, which yields: $s_1 = s_2 = s$. Employing the relation $G = E/[2(1 + \nu)]$ and the elastic moduli of Ni and 3C-SiC specified above, one obtains the following averaged elastic constants of the Ni–3C-SiC nanocomposite: $G = 87$ GPa and $\nu = 0.36$. Although we consider Ni–3C-SiC interphase boundaries as incoherent, we assume that the shear along the interfaces associated with the formation of non-crystallographic dislocations increases the specific interphase energy by $\gamma_{SF\text{-}IB}=m\gamma_{sf}$. Here for a rough estimate of the dependence of γ_{sf} on s, we exploit formula (2), where we put $p = s/b_i$ and $b_i = 0.1$ nm.

Then from formulas (1) and (2) one obtains that, for $\alpha = \pi/4$ and $d = 15$ nm, the dislocation reaction shown in Figs. 6 and 7 occurs at $\sigma_0 > 5.6$–5.8 GPa at $B = 0.7$ nm, and at $\sigma_0 > 9.2$–9.3 GPa at $B = 1.5$ nm (for $m = 0.05$ to 0.2). For the case of a GB crack in the Ni phase, the equilibrium crack lengths are $l_e = 1.7$ nm for $B = 0.7$ nm and $l_e = 7.6$ nm. This means that, as in the case of nanocrystalline Ni, the generation of a GB nanocrack with a length of several nanometers or more in the Ni–3C-SiC nanocomposite requires the formation of a dislocation with the magnitude of the Burgers vector of around 1.5 nm or more. Such dislocations can be generated at ultrahigh stresses, for example, in the course of shock loading.

5. SUMMARY

Thus, we have suggested a mechanism for brittle fracture of solids at ultrahigh stresses arising in the course of shock loading in single-phase and

nanocomposite materials. This mechanism involves homogeneous generation of dislocations with growing Burgers vectors resulting in the formation of dislocations with large Burgers vectors, which, in turn, induce the formation of nanoscale cracks. Such nanocracks can serve as carriers of fracture and promote failure of materials.

ACKNOWLEDGEMENT

This work was supported by the Russian Science Foundation (Research Project 14-29-00199).

REFERENCES

[1] J.D. Kuntz, G.-D. Zhan and A.K. Mukherjee // *MRS Bullet.* **29** (2004) 22.
[2] M. Dao, L. Lu, R.J. Asaro, J.T.M. De Hosson and E. Ma // *Acta Mater.* **55** (2007) 4041.
[3] A. Mukhopadhyay and B. Basu // *Int. Mater. Rev.* **52** (2007) 257.
[4] M. Kawasaki and T.G. Langdon // *J. Mater. Sci.* **42** (2007) 1782.
[5] C.S. Pande and K.P. Cooper // *Progr. Mater. Sci.* **54** (2009) 689.
[6] H.A. Padilla II and B.L. Boyce // *Exp. Mechanics* **50** (2010) 5.
[7] I.A. Ovid'ko and T.G. Langdon // *Rev. Adv. Mater. Sci*. **30** (2012) 103.
[8] L. Lu, M. L. Sui and K. Lu // *Science* **287** (2000) 1463.
[9] M. Chen, E. Ma, K.J. Hemker, H. Sheng, Y.M. Wang and X. Cheng // *Science* **300** (2003) 1275.
[10] M.Yu. Gutkin, I.A. Ovid'ko and N.V. Skiba // *Mater. Sci. Eng.* A **339** (2003) 73.
[11] W.A. Soer, J.T.M. De Hosson, A.M. Minor, J.W. Morris, Jr. and E.A. Stach // *Acta Mater*. **52** (2004) 5783.
[12] S.V. Bobylev, M.Yu. Gutkin and I.A. Ovid'ko // *Phys. Rev.* B **73** (2006) 054102.
[13] D.S. Gianola, S. Van Petegem, M. Legros, S. Brandstetter, H. Van Swygenhoven and K.J. Hemker // *Acta Mater.* **54** (2006) 2253.
[14] F. Sansoz and V. Dupont // *Appl. Phys. Lett.* **89** (2006) 111901.
[15] A.S. Khan, B. Farrok and L. Takacs // *J. Mater. Sci.* **43** (2008) 3305.
[16] S.V. Bobylev, A.K. Mukherjee and I.A. Ovid'ko // *Scr. Mater.* **60** (2009) 36.
[17] S. Cheng, Y. Zhao, Y. Wang, Y. Li, X.-L. Wang, P.K. Liaw and E.J. Lavernia // *Phys. Rev. Lett.* **104 (2010)** 255501.
[18] Y.M. Wang, R.T. Ott, A.V. Hamza, M.F. Besser, J. Almer and M.J. Kramer // *Phys. Rev. Lett.* **105** (2010) 215502.
[19] N.F. Morozov, I.A. Ovid'ko, A.G. Sheinerman and N.V. Skiba // *Rev. Adv. Mater. Sci.* **32** (2012) 75.
[20] V. Taupin, L. Capolungo and C. Fressengeas // *Int. J. Plasticity* **53** (2014) 179.
[21] M.A. Meyers, in: *Dynamic Behavior of Materials* (Wiley, Hoboken, 1994).
[22] M.Yu. Gutkin and I.A. Ovid'ko // *Appl. Phys. Lett.* **88** (2006) 211901; *Acta Mater.* **56** (2008) 1642.
[23] I.A. Ovid'ko and A.G. Sheinerman // *J. Phys.: Condens. Matter* **18** (2006) L225.
[24] I.A. Ovid'ko and A.G. Sheinerman // *J. Phys.: Condens. Matter* **19** (2007) 056008.
[25] I.A. Ovid'ko and A.G. Sheinerman // *Rev. Adv. Mater. Sci*. **27** (2011) 83.
[26] S.V. Bobylev and I.A. Ovid'ko // *Phys. Rev. Lett.* **103** (2009) 135501.
[27] S.V. Bobylev and I.A. Ovid'ko // *Phys. Rev.* B **83** (2011) 054111.
[28] M.Yu. Gutkin, T. Ishizaki, S. Kuramoto and I.A. Ovid'ko // *Acta Mater.* **54** (2006) 2489.
[29] T. Saito, T. Furuta and J.-H. Hwang // *Science* **300** (2003) 464.
[30] X.-L.Wu, Y.T. Zhu and E. Ma // *Appl. Phys. Lett.* **88** (2006) 121905.
[31] U. Kaiser and I.I. Khodos // *Phil. Mag.* A. **82** (2002) 541.
[32] V.L. Indenbom // *Sov. Phys. Sol. State* **3** (1961) 1506.
[33] X. Ma // *Mater. Sci. Eng.* B **129** (2006) 216.
[34] Y. Lin, H., Wen, Y. Li, B. Wen and E.J. Lavernia // *Metall. Mater. Trans*. B **45** (2014) 795.
[35] Y. Lin, B. Xu, Y. Feng and E.J. Lavernia // *J. Alloys and Compounds* **596** (2014) 79.
[36] S.-W. Chang, A.K. Nair and M. Buehler // *Phil. Mag. Lett.* **93** (2013) 196.